



ELSEVIER

Available online at www.sciencedirect.com

SCIENCE @ DIRECT®

Optics Communications 247 (2005) 195–203

OPTICS
COMMUNICATIONS

www.elsevier.com/locate/optcom

Nonlinear polarization evolution: a numerical study of the coupling between main linear normal modes

V. Kermène^a, M.T. Flores-Arias^{b,*}, J. Ares^b,
A. Desfarges-Berthelemot^a, A. Barthélémy^a

^a IRCOM UMR6615, 123 Av. Albert Thomas, 87060 Limoges Cedex, France

^b Laboratorio de Óptica, Departamento de Física Aplicada, Universidade de Santiago de Compostela, Campus Sur, E15782, Santiago de Compostela, España

Received 1 April 2004; received in revised form 3 November 2004; accepted 11 November 2004

Abstract

A numerical modelling of nonlinear changes of polarization by Kerr effect is presented for an optical field propagating along a birefringent silica optical fiber. The kernel of this model comes from expressing the coupled field as a sum of two linear polarization modes in the direction of the fiber principal axes. The developed model is suitable for the design of optoelectronic devices and permits easily taking into account chromatic dispersion, gain or loss, etc.

© 2004 Elsevier B.V. All rights reserved.

PACS: 42.65.Vh; 42.65.Wi; 42.81.Gs

1. Introduction

Intensity-dependent changes of polarization states along a single-mode birefringent fiber [1] have been observed and used for nonlinear pulse reshaping [2,3], light modulation [4], intensity discrimination [5,6], optical logic gate [2] and mode-locking in fiber lasers [7,8]. To build up efficient optical devices, in particular all optical switches,

the intensity variation in transmission with respect to the input intensity, must be as large as possible.

Kerr ellipse rotation (KER) in material exhibiting a cubic nonlinearity, is a well-known phenomenon. It depends on the state of polarization of the input light as well as on its orientation with respect to the birefringence axes if the propagation medium is not isotropic. Polarizing components used in combination with a piece of Kerr material, e.g., a piece of optical fiber, serve usually to create a device with an intensity dependent transmission. The variation in transmission tends to be weaker

* Corresponding author. Tel./fax: +34 981521984.

E-mail address: famaite@usc.es (M.T. Flores-Arias).

as the imbalance between the excited polarization eigenmodes increases [2,9].

In the literature, we note that the most usually adopted model for KER does not predict self-induced polarization changes [2] when the two principal axes of the fiber are equally excited. The assumption made in the model is known as the rotating wave approximation (RWA) [7] and results from neglecting the third order nonlinear coupling between the temporal phases of the main linear modes. However, Winful introduced a more accurate model which took into account nonlinear phase coupling [10]. He demonstrated that nonlinear polarization changes are possible even with equal excitation of the fiber principal axes.

Winful's work lead to an analytical model that describes the propagated optical field as a superposition of two orthogonal circular polarizations. Nevertheless, this model is not always convenient and cannot describe the propagation of short pulses along a nonlinear birefringent fiber because dispersion terms were not included in the analytical approach.

In this paper, we study numerically the propagation considering the optical wave as the superposition of two linear polarization fields propagating along the principal axes of the birefringent fiber and taking into account their complete third order nonlinear coupling.

The main benefits of this method are that: (i) the energy exchange between polarization modes in a linear base is more clearly observed than in a circular one; (ii) the derived expressions are more convenient for modelling of practical situation, and (iii) the formulation allows to introduce the chromatic dispersion effect in such a way that more realistic simulations can be easily performed for short pulse excitations.

The outline of this paper is as follows. Firstly, we write the expressions of the polarization states in terms of the difference in effective indices for the principal linear polarization modes. Secondly, we use these expressions to perform calculations of the polarization changes taking place along a single mode birefringent fiber in various cases. We study the influence of the linear birefringence, the influence of the incident power level and that of the fiber length on the nonlinear polarization

evolution. In all cases, we have considered that the incoming light is linearly polarized at 45° with respect to the principal axes of the fiber.

2. Cross-phase modulation between linear polarization eigenmodes

A lightwave \vec{E} is coupled into a birefringent fiber of length l . The complex electric field vector can be expanded on the basis of the fiber polarization eigenmodes and expressed as a superposition of two linear fields polarized in the direction of the fast (x) and slow (y) fiber axes

$$\vec{E}(x, y, t) = g(x, y)(E_x \hat{x} + E_y \hat{y})e^{-i\omega t}, \quad (1)$$

where $g(x, y)$ is the transverse mode normalized pattern, \hat{x} and \hat{y} are the unitary vectors in the direction of the fast and slow axes, respectively, ω is the angular frequency of the optical field, and t is the temporal coordinate.

The total electric polarization vector is generally expressed as [11]

$$\vec{P}^T = \varepsilon_0 \varepsilon \vec{E}, \quad (2)$$

where ε_0 is the vacuum permittivity and ε is the dielectric tensorial permittivity constant.

The dielectric tensorial permittivity can be expressed as $\varepsilon = (n + n^{\text{NL}})^2$, where n is the linear part of the refractive index and n^{NL} is the change induced by nonlinear effects. If the contribution of the linear refraction is substantially bigger than the nonlinear one ($n \gg n^{\text{NL}}$), we can express the polarization as a sum of a linear and nonlinear contributions as follows:

$$\vec{P}^T \approx \vec{P}^L + \vec{P}^{\text{NL}} = \varepsilon_0 n^2 \vec{E} + 2\varepsilon_0 n n^{\text{NL}} \vec{E}. \quad (3)$$

Furthermore, for an isotropic core fiber, the nonlinear polarization P^{NL} until the third order approximation corresponds to [11]

$$P_i^{\text{NL}}(z, t) = \frac{3\varepsilon_0}{2a_{\text{eff}}} \sum_j \left(\chi_{xyy}^{(3)} E_i E_j E_j^* + \chi_{xyx}^{(3)} E_j E_i E_j^* + \chi_{yyx}^{(3)} E_j E_j E_i^* \right), \quad (4)$$

where $i, j = x$ or y being x, y the fast and slow transversal coordinate indices, E the complex field

amplitude, a_{eff} the fiber effective mode area resulting of $g(x,y)$ integration across the fiber core, $\chi^{(3)}$ the third nonlinear order susceptibility and * denotes complex conjugation. The three independent component of $\chi^{(3)}$, are related by the relation

$$\chi_{xxxx}^{(3)} = \chi_{xyxy}^{(3)} + \chi_{xyyx}^{(3)} + \chi_{yyxx}^{(3)}. \quad (5)$$

In the case of silica fibers the three components have nearly the same magnitude, and we assume they are identical for simplicity.

Combining Eqs. (3) and (4) we derive the following expression for the nonlinear variation of the refractive index as function of the components $E^{(x)}$ of the electric field:

$$n_{(x,y)}^{\text{NL}} = \frac{n_2^{(x,y)}}{a_{\text{eff}}} \left[\left(\left| E^{(x)} \right|^2 + \frac{2}{3} \left| E^{(y)} \right|^2 \right) + \frac{1}{3} \frac{E^{*(x)} E^{(y)}}{E^{(x)}} E^{(y)} \right], \quad (6)$$

where

$$n_2^{(x,y)} = 3\chi_{xxxx}^{(3)}/8n^{(x,y)}$$

is the nonlinear index coefficient. In practice, as the birefringence is small in comparison with the refractive index value, the same value of n_2 can be assumed for both main axes of a silica fiber, so: $n_2 = n_{2(x)} = n_{2(y)} \cong 3.2 \times 10^{-20} \text{m}^2/W$.

We can express the complex components of \vec{E} in polar form:

$$E_x = |E_x|e^{i\varphi_x}, \quad (7a)$$

$$E_y = |E_y|e^{i\varphi_y}, \quad (7b)$$

where φ_x and φ_y denote the input phases.

Then, substituting Eq. (7) in Eq. (6) we obtain new expressions for the nonlinear refractive index depending on the principal axes x, y :

$$n_x^{\text{NL}} = \frac{n_2}{a_{\text{eff}}} \left[\left(|E_x|^2 + \frac{2}{3} |E_y|^2 \right) + \frac{\cos(2\varphi)}{3} |E_y|^2 + i \frac{\sin(2\varphi)}{3} |E_y|^2 \right], \quad (8a)$$

$$n_y^{\text{NL}} = \frac{n_2}{a_{\text{eff}}} \left[\left(|E_y|^2 + \frac{2}{3} |E_x|^2 \right) + \frac{\cos(2\varphi)}{3} |E_x|^2 - i \frac{\sin(2\varphi)}{3} |E_x|^2 \right], \quad (8b)$$

where $\varphi = \varphi_y - \varphi_x$ is the phase difference between the polarization modes.

We emphasize that the nonlinear index Eq. (8) is a complex number. It is straightforward to identify its imaginary term $\alpha^{(x,y)}$ as an amplitude modulation coefficient denoting the energy exchange between the eigenmodes:

$$\alpha^{(x,y)} = (\mp) \frac{2\pi n_2}{3\lambda a_{\text{eff}}} \sin(2\varphi) |E^{(y)}| |E^{(x)}|. \quad (9)$$

Then, a nonlinear birefringence can be defined as

$$\begin{aligned} \Delta n^{\text{NL}} &= \text{Re}(n_y^{\text{NL}} - n_x^{\text{NL}}) \\ &= \frac{2n_2}{3a_{\text{eff}}} \left[|E_y|^2 - |E_x|^2 \right] \sin^2 \varphi, \end{aligned} \quad (10)$$

where Re denotes the real part.

Taking into account the above mentioned equations, we can express the optical field in the vectorial form as follows:

$$\begin{aligned} \vec{E}(z, t) &= |E_x| e^{i\alpha_x^{\text{NL}} z} \hat{x} + |E_y| e^{i\alpha_y^{\text{NL}} z} \\ &\times \exp [i(k(\Delta n^{\text{L}} + \Delta n^{\text{NL}})z + \varphi_0)] \hat{y}, \end{aligned} \quad (11)$$

where φ_0 is an initial phase difference between the input field components, $\Delta n^{\text{L}} = n_y - n_x$ is the linear birefringence of the fiber and $k = 2\pi/\lambda$ with λ the wavelength.

Both the field components and Δn^{NL} depend on z because the accumulated phase difference φ between the main modes changes with the distance. Consequently, the use of a numerical iterative method is necessary to find the value of the electric field in a particular z position.

This aspect of the model that seems a disadvantage compared to the analytical treatment developed in [10], turns out to be a very important advantage in order to achieve a better understanding of the nonlinear ellipse rotation phenomenon. In our model the observation of the interaction between the linearly polarized basic states is possible. Additionally, another important advantage with

respect to the formulation exposed in [10] is that it is straightforward to include extra effects like chromatic dispersion, gain, losses, etc. through a typical split-step numerical method [11].

3. Comments on the nonlinear ellipse rotation phenomenon

We have performed numerical simulations of the behaviour of an optical field propagating down a birefringent single mode silica fiber. Fig. 1(a) shows the flux diagram. The simulated setup is shown in Fig. 1(b).

We focus on the case of a monochromatic wave ($\lambda = 1.550 \mu\text{m}$) linearly polarized at 45° with respect to the principal axes of the fiber (with effective area $a_{\text{eff}} = 80 \mu\text{m}^2$). In this situation $|E_x| = |E_y|$ and $\varphi = 0$ at the entrance of the fiber ($z = 0$).

For a weakly birefringent fiber with $\Delta n^L = 10^{-6}$, Fig. 2 shows the evolution of the nonlinear phase φ_{NL} , the total accumulated phase φ and the amplitude of the polarization modes, $|E_x|$, $|E_y|$, along one beat length $L = \lambda/\Delta n^L$ [11]. The wave propagates oscillating along the x and y components. Because of the linear birefringence, the components are soon out of phase ($\varphi \neq 0$). This phase difference in turn induces an energy exchange between the field components through the modulation coefficients $\alpha \begin{pmatrix} x \\ y \end{pmatrix}$. Next, that transfer increases in turn

the nonlinear phase contribution (see Eq. (10)). The process continues during propagation until the total phase φ (Fig. 2(b)) is such that the nonlinear phase φ_{NL} (Fig. 2(a)) is back to zero. During this cycle of evolution, the field components exchange energy (Fig. 2(c)). Then a new cycle of evolution begins.

Analyzing the polarization behaviour we can identify two extreme cases. The first corresponds to the case where the nonlinear contribution to the birefringence is small in comparison with the linear one. In that situation the polarization rotation is weak. The more important contribution of the linear birefringence to the total accumulated phase forces the instantaneous nonlinear phase to have a short oscillation period as well as a weak

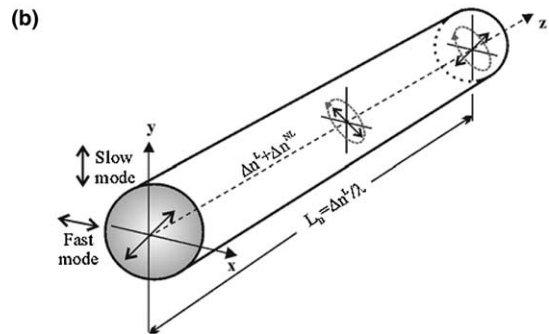
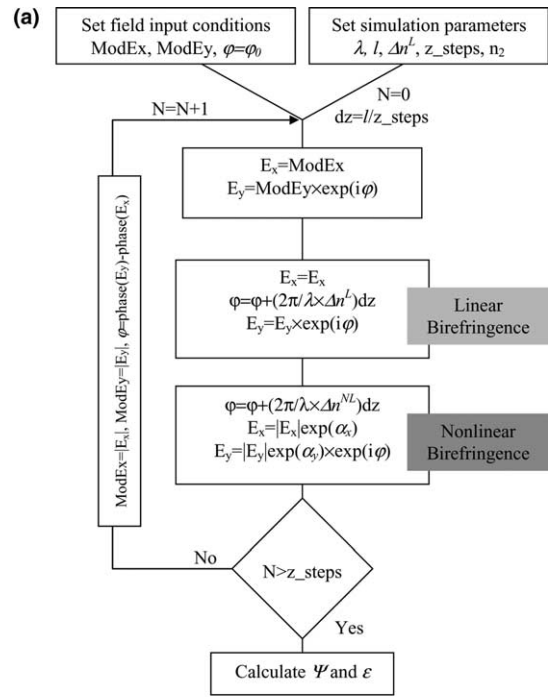


Fig. 1. (a) Algorithm diagram of the numerical simulation to calculate the azimuth angle ψ and ellipticity ϵ of the polarization state. z_steps corresponds to the number of z samples. (b) Represents the simulated system.

amplitude as the wave propagates along the fiber. So, the nonlinear polarization evolution is negligible for realistic input power values. Nevertheless it is important to note that a nonlinear behaviour can be reached because of the total accumulated nonlinear phase for practical input powers if the fiber is chosen long enough. In practice, the signature of this nonlinear effect could be masked by fiber losses, fiber twist [12,13], fiber bending [14], or temporal effects [11].

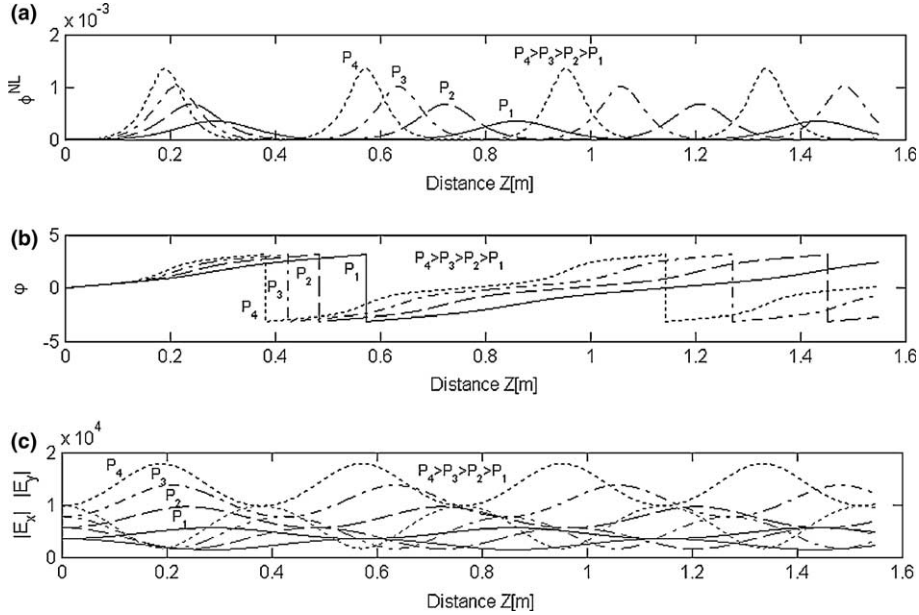


Fig. 2. Evolution of: (a) the phase non linear ϕ^{NL} , (b) the total accumulated phase ϕ and (c) polarization mode amplitudes $|E_x|, |E_y|$ versus z over one fiber A beat length. We can see superimposed the plots for four different input powers. Calculations have been made for $a_{\text{eff}} = 80 \mu\text{m}^2$ and $P_1 = 7000 \text{ w}$, $P_2 = 11167 \text{ w}$, $P_3 = 15333 \text{ w}$, $P_4 = 19500 \text{ w}$.

The second extreme case occurs when the nonlinear birefringence is larger than the linear birefringence. In that situation, the field rotation can be clearly observed for realistic input power levels. Additionally the fiber does not need to be extremely long to generate a significant nonlinear phase contribution. The model described in this work confirms these results [5]. As can be seen in the simulated case exposed in Fig. 2, for weakly birefringent fibers the nonlinear phase term takes a non null value during an important part of the propagation. In that situation, the linear phase difference grows up slowly and the nonlinear phase difference contribution overcomes the linear one very quickly.

4. Study of some particular cases

As a first case, for a better comparison with the results presented by Winful in [10], we consider different birefringent fibers of length equal to their respective beat lengths. All fibers have the same effective area.

For an input field linearly polarized at 45° and $\lambda = 1.550 \mu\text{m}$, Fig. 3 shows the corresponding azimuth (Ψ) and ellipticity (ϵ) of the elliptic polarization state at the fiber output [15] versus the input power. The solid curves correspond to a wave which travelled along a fiber A with birefringence $\Delta n_A^L = 10^{-6}$, during one beat length. The dashed and dotted curves correspond to fiber B ($\Delta n_B^L = 5 \times 10^{-5}$) and fiber C ($\Delta n_C^L = 10^{-4}$), respectively, with a propagation length equal to their respective beat length $L_B = \lambda/\Delta n_B^L = 31 \text{ mm}$ and $L_C = \lambda/\Delta n_C^L = 15.50 \text{ mm}$.

If we compare the different curves we confirm that nonlinear polarization changes can be more easily observed for weakly birefringent fibers [11] $\Delta n_A^L = 10^{-6}$ since, a higher input power is required for achieving a similar behaviour in a fiber of larger birefringence. These conclusions are in agreement with the results presented in [10]. Note that, in the balanced excitation of eigenmodes considered here, it is possible to find an input power leading to a full polarization switching (point F) corresponding with the solid curves.

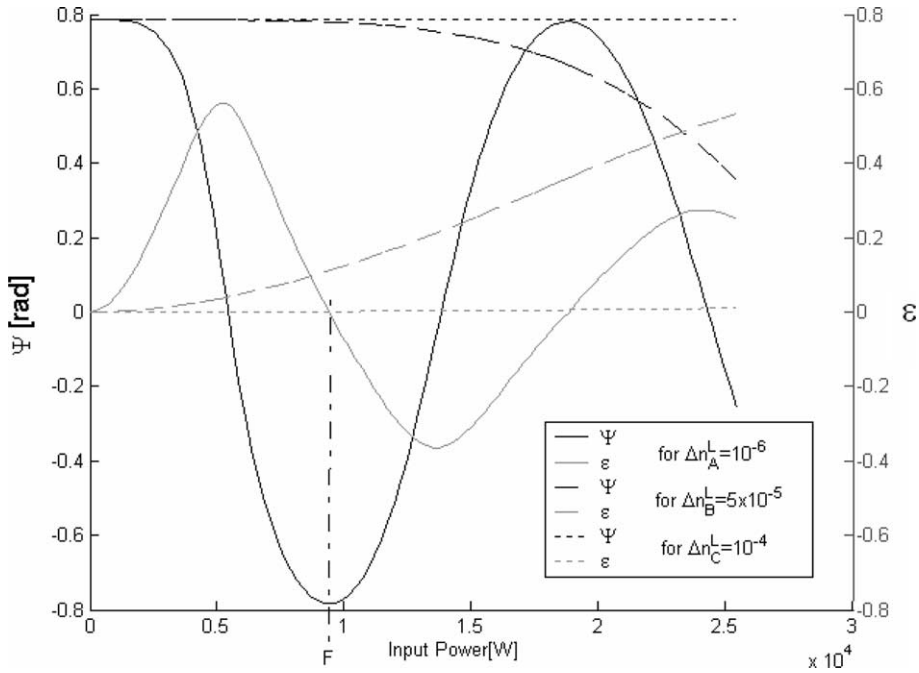


Fig. 3. Ellipticity ε - (plotted in grey) and azimuth ψ - (plotted in black) of the polarization ellipse of the transmitted wave at the end of a beat length, versus input power P . Solid curves correspond to $\Delta n_A^L = 10^{-6}$, dashed curves to $\Delta n_B^L = 5 \times 10^{-5}$ and dotted curves to $\Delta n_C^L = 10^{-4}$. F corresponds to the operating point where full polarization switching is reached for fiber A.

As a second case, we have looked for the power P_C necessary to reach, in a highly birefringent fiber (with Δn_C^L), the same polarization changes as the one obtained in a low birefringent fiber (Δn_A^L) for an input power P_A (Fig. 4). We found from various set of simulations the following scaling law:

$$P_C = \frac{\Delta n_C^L}{\Delta n_A^L} P_A. \tag{12}$$

The fiber length was maintained equal to one beat length. The above expression indicates that, provided we change the input power by a factor ($\Delta n_C^L / \Delta n_A^L$), a birefringent fiber C of length equal to its beat length L_C would present exactly the same polarization behaviour than a fiber A with linear birefringence (Δn_A^L) of length equal to L_A .

Now by means of a new set of simulations, we wanted to answer the following question: knowing the polarization changes that we got with a birefringent fiber A of linear birefringence Δn_A^L and ac-

tual length L_A , is it possible to find the length of fiber D with birefringence (Δn_D^L) giving a similar behaviour for identical input powers?

With respect to the previous calculations we kept the same linearly polarized input and we observed the polarization modifications induces by fibers with different lengths and birefringences. To avoid confusion between beat length and actual length, the last one will be denoted henceforth by l . When $\Delta n_D^L > \Delta n_A^L$, it is clear that for the same input power, we need a fiber D longer than fiber A so that the propagating wave accumulates a similar nonlinear phase. Fig. 5 shows that for a fiber D of birefringence $\Delta n_D^L = 10^{-5}$ a length l_D 3.8 times longer than L_A is enough to obtain a similar polarization state at the output. In terms of the beat length of the fiber D this means that we need a fiber 380 times longer than its beat length L_D . Looking to a new sample, corresponding to fiber E with $\Delta n_E^L = 0.7 \times 10^{-4}$, we need $l_E = 22.26 \times L_A$ to obtain an identical output for the same power

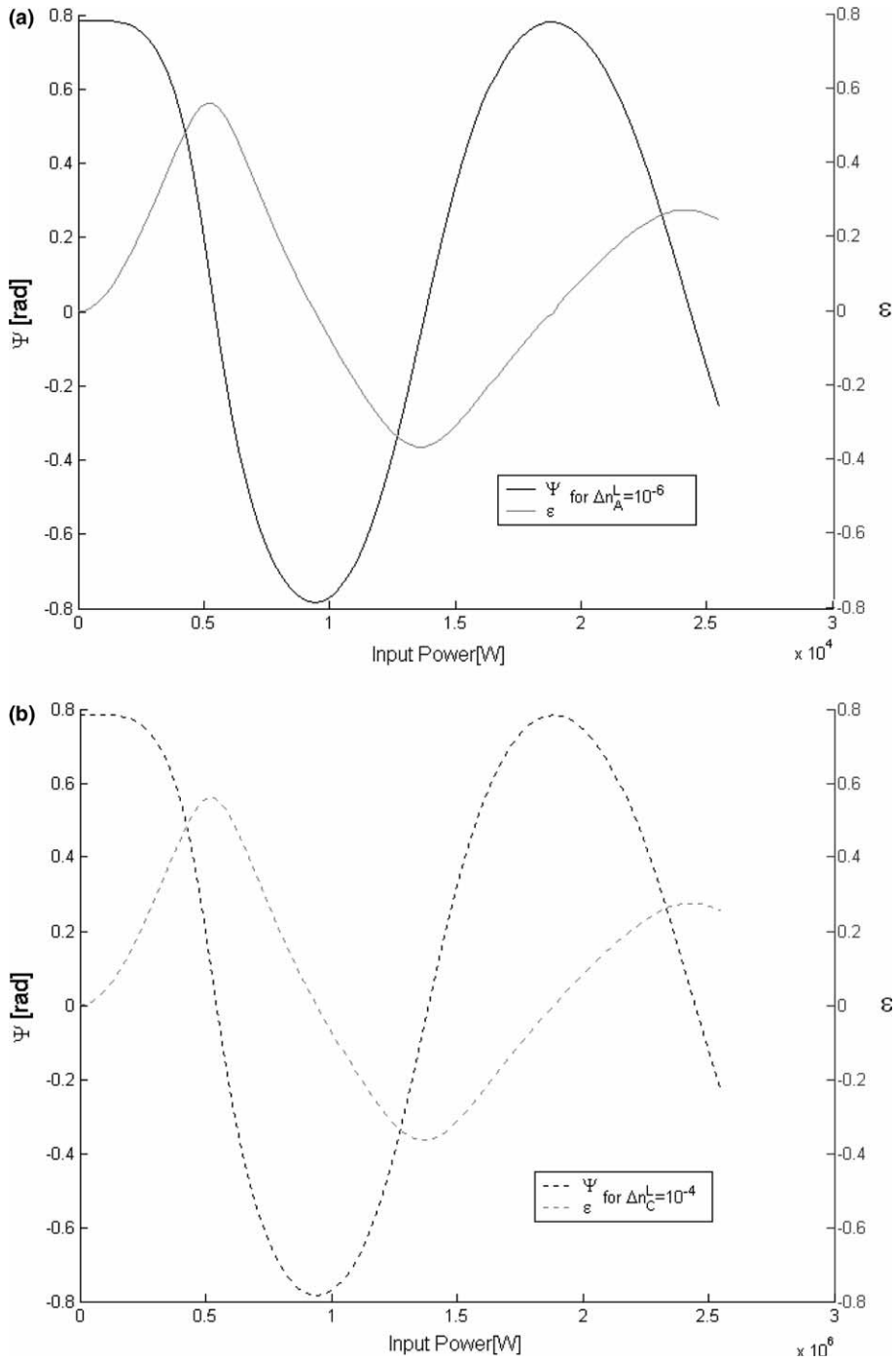


Fig. 4. Ellipticity ϵ - (plotted in grey) and azimuth ψ - (plotted in black) of the polarization ellipse of the transmitted wave at the end of one beat length, versus input power P : (a) $\Delta n_A^L = 10^{-6}$, (b) $\Delta n_C^L = 10^{-4}$. Note that the power axis scale is two orders of magnitude higher ($\Delta n_C^L/\Delta n_A^L$) in the second graph.

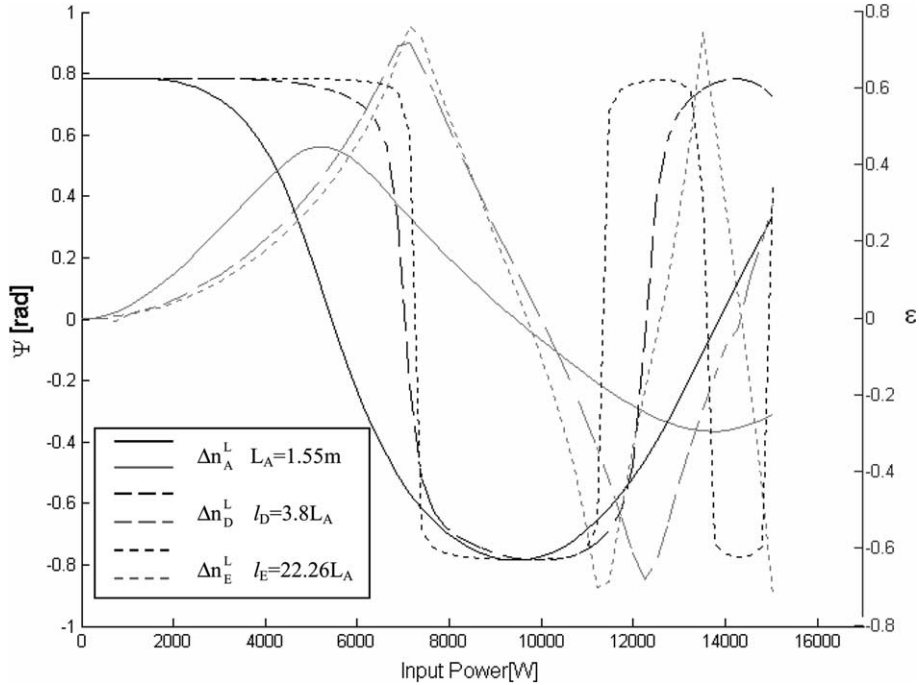


Fig. 5. Ellipticity ε - (plotted in grey) and azimuth ψ - (plotted in black) of the polarization ellipse of the transmitted wave at the end of different fibers, versus input power. Solid curves correspond to $\Delta n_A^L = 10^{-6}$, $L_A = 1550$ mm, dashed curves to $\Delta n_D^L = 10^{-5}$, $I_D = 3.8 \times L_A$ and dotted curves to $\Delta n_E^L = 0.7 \times 10^{-4}$, $I_E = 22.26 \times L_A$.

level. As expected, the greater the birefringence the longer the required fiber length for achieving a similar nonlinear polarisation evolution. We note, however, that it is difficult to achieve a full coincidence between the power dependent traces as the difference between the two linear birefringences gets large. For instance the steepness of the polarisation switching increases for large birefringence.

5. Conclusions

We have modelled the third order nonlinear interaction between the two linearly polarized modes of a birefringent silica optical fiber. The derived equations are more correct than the standard ones and include the nonlinear coupling occurring when the two principal axes of the fiber are equally excited. They are well suited to the investigations and modelling on nonlinear polarisation evolution. We have identified the successive and peri-

odic energy exchange between the fast and slow linear modes of the fiber as the more significant result of the interaction between the linear and nonlinear birefringence.

Taking advantage of the derived expressions, we have simulated the propagation of a linearly polarized field launched at 45° with respect to the main axes of a singlemode birefringent fiber. That configuration is the most suitable to obtain a highly contrasted polarisation switching. The model shows how the modal power exchange leads to the mutual birefringence interaction during the propagation of the input field. We have compared the propagation along one beat length in different type of fibers for a fixed power. As expected, the smaller the linear birefringence the more important the polarization changes. Higher powers are necessary to achieve the same nonlinear polarisation evolution in highly birefringent fibers by reference to low birefringence fibers. We have demonstrated that the power scaling is directly

proportional to the birefringence ratio. The chance of achieving similar nonlinear polarization changes at the exit of different birefringent fibers by propagating the optical field on a longer distance was investigated. In particular, we have shown that the same polarization changes can be achieved with two different fiber pieces which birefringence differs by one order of magnitude after proper choice of their respective length. Finally we want to stress that losses, twists, random defects [16] and chromatic dispersion effects in the fiber can be easily introduced in the calculations through a similar iterative split-step method, to carry on simulation closer to reality and to consider short pulse excitations.

Acknowledgements

This study was partially supported by the Ministerio de Educación y Ciencia, Spain, under contract TIC 2003-03041. M.T. Flores-Arias and J. Ares acknowledge the researching grant of the Xunta de Galicia, which made possible their collaboration in this work.

References

- [1] C.R. Menyuk, *Opt. Lett.* 12 (1987) 614.
- [2] R.H. Stolen, J. Botineau, A. Ashkin, *Opt. Lett.* 7 (1982) 512.
- [3] M. Horowitz, Y. Silberberg, *Opt. Lett.* 22 (1997) 1760.
- [4] J.M. Dziedzic, R.H. Stolen, A. Ashkin, *Appl. Opt.* 20 (1981) 1403.
- [5] B. Nickolaus, D. Grischkowsky, A.C. Balant, *Opt. Lett.* 8 (1983) 189.
- [6] H.G. Winful, A. Hu, *Opt. Lett.* 11 (1986) 668.
- [7] M. Hofer, M.E. Fermann, M.E. Haberl, M.H. Ober, A.J. Schmidt, *Opt. Lett.* 16 (1991) 502.
- [8] H.A. Haus, E.P. Ippen, K. Tamura, *IEEE J. Quant. Electron.* 30 (1994) 200.
- [9] M.E. Fermann, M.J. Andrejco, Y. Silberberg, M.L. Stock, *Opt. Lett.* 18 (1993) 894.
- [10] H.G. Winful, *Appl. Phys. Lett.* 47 (1985) 213.
- [11] G.P. Agrawal, *Nonlinear Fiber Optics*, Academic Press, London, 1989 (Chapters II, III and VII).
- [12] J. Ullrich, A. Simon, *App. Opt.* 18 (1979) 2242.
- [13] C.R. Menyuk, P.K.A. Wai, *JOSA Councm.* 11 (1993) 1305.
- [14] M. Nakazawa, T. Nakashima, S. Seikai, *Appl. Phys. Lett.* 45 (1984) 823.
- [15] M. Born, E. Wolf (Eds.), *Principles of Optics*, sixth ed., Pergamon, Oxford, 1980 (Chapter I).
- [16] M.F. Arend, M.L. Dennis, I.N. Duling III, E.A. Golovchenko, A.N. Pilipetskii, C.R. Menyuk, *Opt. Lett.* 22 (1997) 886.